Finite Element Modeling of Elastic Modulus in Ductile Irons: Effect of Graphite Morphology

S.H. Pundale
R.J. Rogers
G.R. Nadkarni
University of New Brunswick
Fredericton, New Brunswick, CANADA

ABSTRACT

This investigation is the first to deal with the modeling and prediction of effective elastic modulus of ductile irons using finite elements. Both plane stress and axisymmetric formulations were used to predict elastic moduli. With finite elements, it is possible to include microstructural parameters that are extremely difficult or impossible to model analytically. Assuming that the graphite nodules act as voids, the effective elastic modulus was modeled by considering the effect of small strains for nodule variables of volume fraction, shape, size and distribution. (No matrix variables have been considered.)

It was seen that graphite volume fraction significantly affects the elastic modulus. For a given volume fraction, it was also seen that nodule shape has a significant effect on the modulus. Analytical modeling, based on existing literature sources, was also used to predict effective moduli; the Mori-Tanaka model was found to give reasonable predictions.

INTRODUCTION

Ductile iron consists of spheroidal graphite nodules embedded in matrices such as ferrite, pearlite, tempered martensite or austenite. Austempered ductile irons (ADI), with their ausferritic matrix microstructure, are a recent addition to the ductile iron family. The mechanical properties of ADI are directly comparable to that of forged steel components.[1] However, the elastic modulus (Young's modulus) of the best made ductile irons is about 10–15% lower than that of steels. This has made mechanical designers wary of using ductile iron components, especially in cases where stiffness is an important criterion. The lower elastic modulus of ductile irons is one of the major stumbling blocks for designers interested in harnessing the excellent combination of properties (high strength/weight, high damping capacity, easy manufacturability) offered by this unique family of materials.

In order to utilize the complete potential of ductile irons, it is necessary to gain an intimate understanding of their effective elastic modulus in terms of their microstructural parameters. Such an understanding would contribute to further enhancing the competitiveness of ductile irons.

Elastic Modulus in Cast Iron

Elastic modulus is a fundamental material property that represents the inherent stiffness of the material. It depends primarily upon atomic bonding, the crystallographic structure, the composition and the microstructure of the material. These influences for ductile irons are shown schematically in Fig. 1.[2] (Note that, in this paper, the terms elastic modulus and modulus are used interchangeably and should not be confused with foundry terminology such as casting modulus or section modulus.)

Elastic modulus can be measured by static and dynamic methods. Static methods involve determining the slope of the stress-strain curve obtained from a conventional uniaxial tensile test coupon using extensometers or strain gauges. Dynamic methods, such as resonance and pulse echo, are among the most commonly used techniques to determine the dynamic elastic modulus (DEM). They are preferred over static methods, due to the relative ease of sample preparation and their greater precision. In the case of homogeneous materials, such as steels, the static and dynamic moduli agree within the uncertainty of the static measurements.[3,4]

Several studies have shown that the elastic modulus is primarily affected by graphite volume fraction and nodule shape.[5–7] Secondary effects, due to matrix variables (matrix microstructure, alloying solid solution elements, precipitates, grain size, segregation), are less important.

Early work by Plenard considered the effect of graphite on elastic moduli in gray cast irons.[5] Many studies have independently established that the modulus decreases as the volume fraction of graphite (V_g) increases.[5,8,9] Decreasing V_g by a maximum of ~3% could increase the modulus by ~4.5% over the base composition. The elastic modulus significantly increases as the shape of graphite changes from flaky to nodular for the same volume fraction of graphite.[5]

Speich et al.[6] measured the DEM of gray and nodular cast irons and analytically modeled the effect of graphite shape on the elastic modulus. A lower value of modulus was reported for flaky graphite corresponding to gray irons. In ductile irons, the modulus decreases as the nodularity decreases; a decrease in nodularity of ~10% is sufficient to decrease the DEM by ~5%.[10]

Kovacs and Cole[8] conducted a systematic study of the effect of section sizes and carbon content on DEM in pearlitic ductile irons. They showed that an increase in section size decreased the moduli.

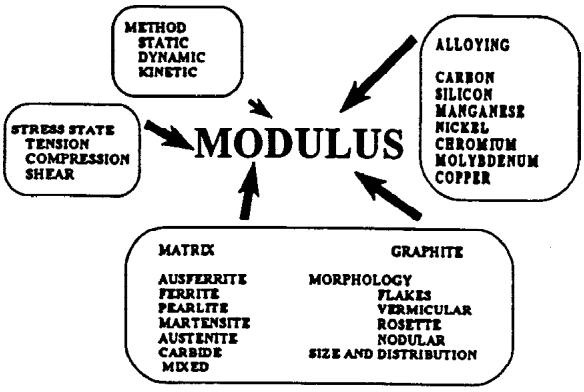

Fig. 1. Factors affecting the elastic modulus in ductile irons.

Since larger section size corresponds to slower solidification rates and, indirectly, to increased nodule size, the elastic modulus was shown to decrease as nodule size increased.

Not much work has been undertaken to show the effect of graphite distribution on the modulus. In recent years, Shi et al.[7] have studied the effect of graphite elongation on mechanical properties. It was shown that the elastic modulus in the rolled direction increased as the rolling reduction increased. This clearly shows that graphite orientation effects are important when ductile iron is worked.

Modeling Elastic Modulus

To model the DEM of ductile irons analytically, ductile irons could be considered as a composite material that contains a weak inclusion (spheroidal graphite of uniform shape, size and distribution) in a strong, uniform and homogeneous matrix. The analytical methods are broadly grouped into the following categories: mechanics of materials, variational approach (or bounding) and mean-field theory.

Analytical modeling requires estimated values for the elastic modulus of the components of the matrix material. Dryden et al.[11] in their work on the effect of graphite in cast irons used 208 GPa as the elastic modulus of the matrix. Speich et al.[6] studied the elastic modulus of ductile and gray irons as a function of graphite volume fraction. By extrapolating to a zero volume fraction, they obtained 209 GPa as the elastic modulus of ferrite. This is the matrix value used in the present work.

Estimates of the elastic modulus of graphite vary considerably (e.g., 8 GPa[6] to 686 GPa[12]). Using nanoindentation of ferritic ductile irons, Dierickx et al.[13] found graphite modulus values of 15 ±5 GPa. The present work uses 15 GPa, as this correlates well with most experimental and analytical studies. Due to the large difference between the modulus values of graphite and ferrite, reasonable results can also be obtained by treating the graphite nodules as voids.

In one of the simplest cases of the mechanics of materials approach (Rule of Mixtures), each component contributes to the modulus in a quantity directly proportional to its volume fraction. Hashin and Shtrikman[14] developed stringent bounds using a variational approach to predict the modulus for a composite material that is, in a statistical sense, isotropic and homogenous. The model fails for the extreme case, where the particulate is much stiffer than the matrix, in which case the upper bound becomes infinity. This model was used to analytically model the elastic modulus of ductile irons by Plenard[5] and Speich et al.[6] Good agreement with the experimental results was reported in both works.

Mori and Tanaka[15] were among the first to suggest a mean field theory model, which is valid for low modulus inclusions, as well as for pores. For two-phase systems, with appropriate assumptions, the Mori-Tanaka model predicts the modulus with sufficient accuracy.

Analytical models for predicting the effective elastic response of composites are usually based upon assumptions of uniform spatial distribution and idealized geometrical shapes of the second phase and can, therefore, provide erroneous predictions of the overall elastic response for real composite materials, in which the shape and distribution of the second phase particles are seldom uniform. Finite element analysis (FEA) can be used to examine the effects of second-phase morphology on elastic modulus in greater detail. This is the purpose of the present work.

MODEL FORMULATION

Wang et al.[16] have proposed an analytical model for the effective modulus for periodically distributed circular and elliptical voids. They modeled a single ellipsoidal void for plane stress conditions. Shen et al.,[17] in their work on the effective elastic response of a two-phase composite, have proposed a similar model for plane stress, plane strain and axisymmetric conditions.

In order to formulate the finite element model, the following assumptions were made regarding the microstructure of ductile iron:

1. The ausferritic matrix is assumed to be uniform and homogeneous without any segregation.
2. There are no carbides present and the alloy content is distributed uniformly.
3. Graphite behaves like a void, and its elastic modulus is therefore considered to be zero.
4. Graphite morphological parameters of shape, size and distribution act independently.

The minimum roundness for which graphite is considered nodular is 65%. There are two ways to model the effect of decreasing roundness. Decreasing the ratio of the semi-major axis (a) to semi-minor axis (b) from 1 to 0.25 changes the roundness from 100% to 64%. Hence, the effect of shape can be modeled by considering various b/a ratios. A schematic of this can be seen in Fig. 2.

Another way to vary the roundness is to increase the surface irregularity for the same b/a ratio. The effect of irregularity can be modeled by considering either sinusoidal or triangular surface waveforms. The effect of nodule size for the same volume fraction can be assessed by considering multiple nodules of decreasing radii.

Consider the symmetry of a quarter of an isolated cell (Fig. 3), which has the following boundary conditions used by Wang et al.:[16]

$$\begin{aligned} &\Gamma_0 : \frac{x^2}{a^2} + \frac{y^2}{b^2} = 1 \quad \sigma_t = \sigma_n = 0 \\ &\Gamma_1 : y = L \quad \sigma_t = 0 \quad u_n = \bar{u}_n \\ &\Gamma_2 : x = L \quad \sigma_t = 0 \quad u_n = d \end{aligned} \tag{1}$$

where subscripts n and t denote the normal and shear components of boundary traction or displacement on surfaces Γ_0, Γ_1, and Γ_2. Stress is induced by the unit positive normal displacement $\bar{u}_n$ on Γ_1. The effect of Poisson's ratio results in a negative displacement, d, on Γ_2, which is prescribed as uniform.

For a plane stress model,[16] if the negative normal displacement, d, is chosen such that $\int_\Gamma \sigma_n \, d\Gamma = 0$ on boundary Γ_2, then the elastic modulus in the vertical direction is defined as:

$$E_1 = \frac{\int_{\Gamma_1} \sigma_n \, d\Gamma}{\bar{u}_n} \tag{2}$$

Although the plane stress model is easy to formulate and compare with the analytical results,[16] a 2-D axisymmetric model should be a better representation of an ellipsoidal nodule.

For the axisymmetric case, the elastic modulus is given by:[17]

$$E_1 = \frac{2L_0}{R_0^2} \frac{\int_0^{R_0} \sigma_n r \, dr}{\bar{u}_n} \tag{3}$$

Again, normal traction is given on surface Γ_1. The parameters L_0 and R_0 denote the height on the Y-axis and the radius of the X-axis, respectively. In the case considered in Fig. 3, L_0 equals R_0 and is given by L. $\bar{u}_n$ is the displacement in the Y direction.

FINITE ELEMENT MODELING

Finite element modeling (FEM) was done using ANSYS™ (v5.2) on a SUN SPARC IPX workstation networked with a SPARC1000 server. The geometry was modeled using the UNIGRAPHICS™ (v10 and v11) CAD system. The IGES file transfer protocol was used to transfer the model into ANSYS™. The ANSYS input file can be divided into three distinct sections, which will be discussed in the following text.

In the first section, the body geometric constants are initially defined (e.g., L = 10 units). The IGES file is then imported, and key points and important nodal points are defined. The final geometry is defined by subtracting the nodule areas when they are treated as voids. Meshing is then carried out after defining the element size near critical lines. Element size is defined as being smaller around the voids and slightly larger along the boundaries. A unit value is prescribed for the elastic modulus, and Poisson's ratio is d/L, where an initial value for d is assumed. The 8-node PLANE82 elements are used to mesh the geometry. Depending on the geometry, both plane stress and axisymmetric cases were considered. Figure 4 shows sample mesh.

Matrix computations to obtain the elastic modulus for the given geometry are defined in the second section of the input file. Boundary conditions are prescribed, as shown in Fig. 3. Symmetry conditions are placed along the coordinate axes. An initial solution is then obtained for the assumed value of the negative displacement, d.

The X and Y components of stresses are computed on sides Γ_1 and Γ_2, and the following stress integrals are defined:

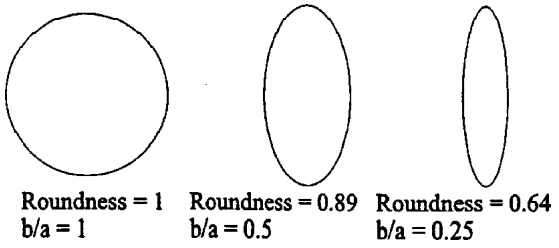

Fig. 2. Roundness values for various b/a ratios.

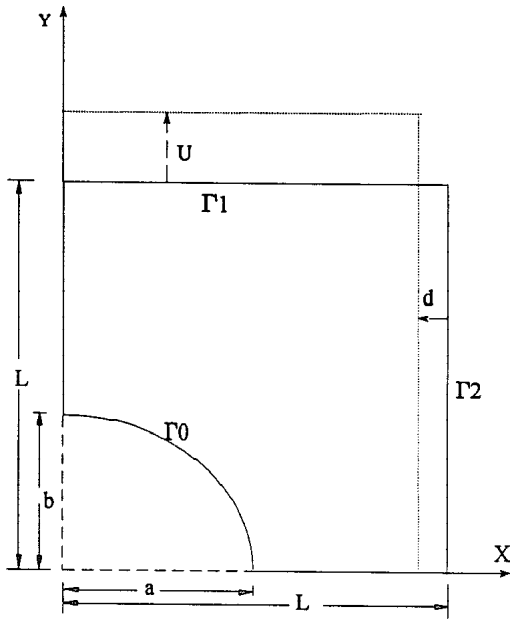

Fig. 3. Nodule quarter symmetry for finite element modeling.

$$\begin{aligned} \gamma_{1x} &= \left| \int_{\Gamma_1} \sigma_x d\Gamma \right| \\ \gamma_{1y} &= \left| \int_{\Gamma_1} \sigma_y d\Gamma \right| \\ \gamma_{2x} &= \left| \int_{\Gamma_2} \sigma_x d\Gamma \right| \\ \gamma_{2y} &= \left| \int_{\Gamma_2} \sigma_y d\Gamma \right| \end{aligned} \qquad (4)$$

The sum of tangential stresses on the surfaces, γ_{tan}, is then defined such that $\gamma_{tan} = \gamma_{1x} + \gamma_{2y}$. Since both γ_{2x} and γ_{tan} have to be minimized to fulfill the boundary conditions,[16] an optimization variable, B, is defined such that $B = \gamma_{2x} \times \gamma_{tan}$. The negative displacement, d, is optimized by an optimization routine in ANSYS™ such that B is minimum, i.e., both γ_{tan} and γ_{2x} are minimal or near zero. Convergence was typically observed after 10 steps.

It was observed that the variable γ_{2y} does not contribute significantly to the value of the optimization variable, since it is not actually the surface tangential stress. Hence, it is possible to redefine the variable γ_{tan} equal to γ_{1x} alone. There was only 0.01% difference in the values of elastic modulus as a result of this change.

In the third section, post-processing is the final step and is done after the optimization is complete. The effective elastic modulus is determined as the integral of the Y component of stress on side Γ_1 with respect to X, i.e., γ_{1y}. Using the same geometry and mesh, values for the elastic modulus in the X direction are obtained by simply putting a positive unit normal displacement on Γ_2 and optimizing the negative displacement on Γ_1.

MODEL VALIDATION AND SENSITIVITY

The results obtained by the finite element method have been compared to the published results by Wang et al. for plane stress.[16] The published results showed the values of E_1, the normalized modulus along the Y-axis, and E_2, the normalized modulus along X-axis, as a function of void volume fraction (L/a ratio) for given b/a ratios (where b/a indicates the ratio of the semi-major to the semi-minor axes). As expected, it was found that E_1 and E_2 increased as the volume fraction decreased. As well, E_1 increased with increasing b/a ratios, where b is along the Y-axis. As seen in Fig. 5 for b/a = 0.75, the maximum difference between the values of E_1 (or E_2) obtained by FEM and the corresponding published value of E_1 (or E_2)[16] is less than 1%.

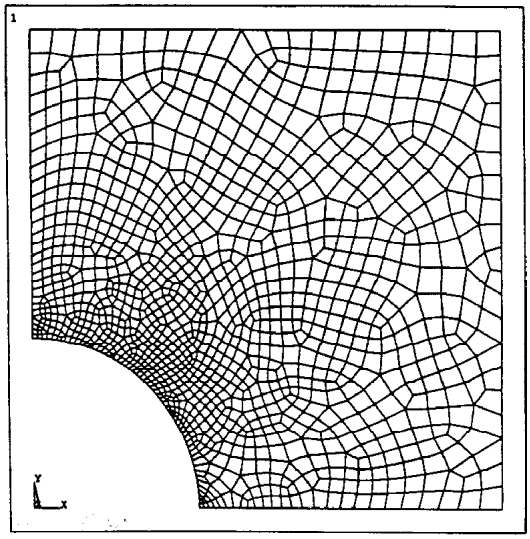

Fig. 4. Typical finite element mesh.

The sensitivity of the model was then observed by varying geometric and other parameters and observing the differences. Using $\bar{u}_n = 2$ or $\bar{u}_n = 0.5$, a 2% difference was noted, as compared to the published value of E_1.[16] Therefore, it is concluded that doubling or halving the displacement produced no significant change in the results. Doubling or halving all dimensions resulted in a 0.03% difference in the modulus values.

It was shown that, for the trivial case where a = b = 0 (no void), the value of the moduli $E_1 = E_2 = 1$. It was seen that the E_1 and E_2 values were complementary. The value of E_1 at b/a = 2.5 is the same as the value of E_2 at b/a of 0.4 (the reciprocal of 2.5). Two meshes of varying element size were examined (402 and 1004 elements) and it was observed that variation in the element size did not lead to a significant change in the value of the modulus obtained.

To see the effect of the non-zero graphite modulus, the area of the void was meshed and given an elastic modulus equal to the ratio of the graphite and matrix moduli. The boundary between the graphite and matrix was assumed to be perfectly bonded. This is simple to model and gives an upper bound estimate of the effective modulus. Symmetry boundary conditions were used on the axes of symmetry.

The same values of Poisson's ratio (d/L) was used for the graphite.[6] The effective modulus due to graphite was then obtained as a function of volume fraction for the axisymmetric case with spherical nodules, and the results compared to the case where voids were assumed. Figure 6 shows that there is no significant difference between the two results over the range of volume fractions examined. The use of voids in the analysis is therefore justified.

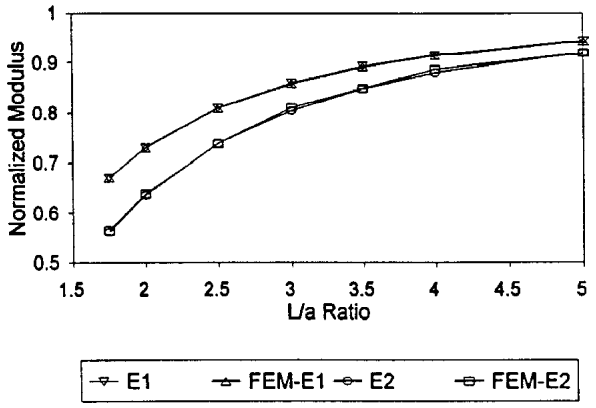

Fig. 5. Normalized finite element modulus values for plane stress with published results by Wang et al.[16] for b/a = 0.75.

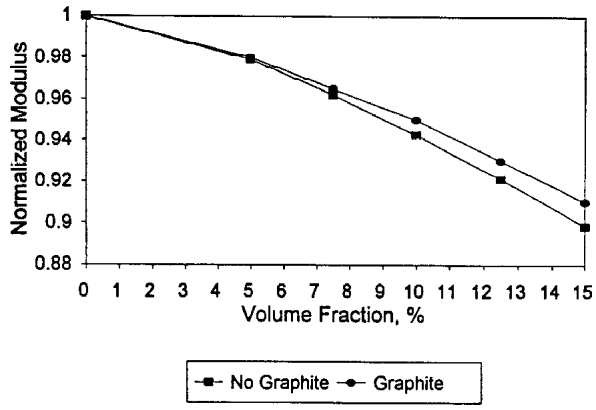

Fig. 6. Results justifying the assumption that nodules can be modeled as voids.

RESULTS AND DISCUSSION

Primary Effect—Volume Fraction

Graphite volume fractions for ductile irons range from 5–15%, with the most commonly used range being 8–12%. The effect of void volume fraction on the calculated elastic modulus is shown in Fig. 7 for values up to 15%. The finite element results are for circular voids and elliptical voids with b/a = 0.5. The effective modulus predicted as a result of the analytical approaches is also considered, as well as some experimental data points.

As anticipated, the predicted modulus decreases as the void volume fraction increases. The plane stress finite model is seen to roughly predict a lower bound for the value of effective modulus, whereas the axisymmetric model gives very high values. A perfectly circular and smooth void geometry was assumed for the finite element modeling. Ductile irons could contain up to 35% highly irregular nodules, which could lead to a significant drop in the modulus.

If the combined effect of these geometries are considered in the modeling, this will lead to decreases in the values of modulus predicted for both plane stress and axisymmetry. It is expected that, in this case, the predictions obtained by the axisymmetric model would be closer to the experimental values.

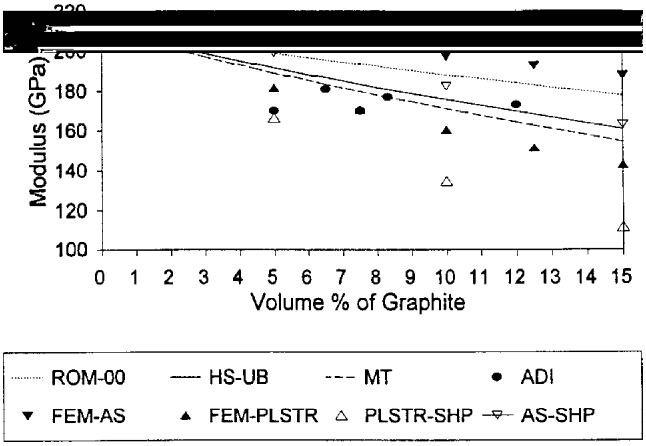

Fig. 7. Effective modulus as a function of graphite volume fraction for plane stress and axisymmetry, along with results from analytical models and experimental data; note the differences in the FEM results for circular voids (filled triangles) and for elliptical voids with b/a=0.5 (empty triangles).

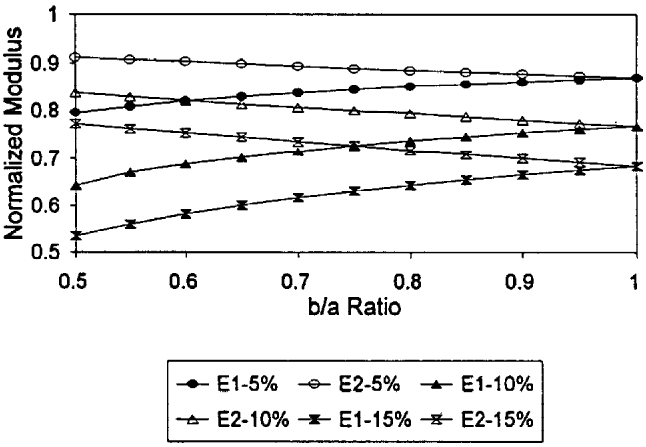

Fig. 8. Effect of ellipse axis ratio for plane stress.

Compared to the experimental data obtained from DEM measurements, it is seen that, for the analytical models, the Rule of Mixtures gives rather high predictions for the value of modulus. Rule of Mixtures underestimates the reduction in modulus due to graphite volume fraction by roughly 50%. The Hashin-Shtrikman upper bound prediction is lower than the values predicted by Rule of Mixtures, and closer to the experimental data. The Mori-Tanaka model is seen to give a reasonable prediction for the value of the modulus.

Secondary Effects—Shape, Size, Distribution

For a given volume fraction of void, the effect of nodule shape, size and distribution on the elastic modulus were also studied.

Nodule Shape

The effect of graphite shape was studied for both plane stress and axisymmetric situations. The effect of different ellipse axis ratios on the normalized modulus is shown in Fig. 8 for the plane stress model for volume fractions of 5, 10 and 15%. The shapes varied from a circle to an ellipse with a decreasing b/a ratio down to 0.5. It is shown that the modulus in the tensile direction, E_1, increases as the b/a ratio increases. E_2 can be considered as the modulus where the tensile direction is the X-axis; it is shown to decrease with increasing b/a ratios. It is also seen that an increasing volume fraction leads to an increasing difference between E_1 and E_2 at lower b/a ratios, implying a significant increase in anisotropy.

For the axisymmetric model, the effect of void shape on the normalized modulus can be seen in Fig. 9, where the complementary b/a values are used. The tendency is the same as that of the plane stress model, although the actual modulus values are higher.

Nodule Size

To study the effect of nodule size, the volume fraction of the second phase particles is kept constant, but the surface area-to-volume ratio, S_v, is increased by increasing the number of particles. Multiple particles can only be modeled using plane stress. The effect of size was investigated for a constant volume fraction of 10%. No significant effect was observed for plane stress for increases in the S_v values by a factor of four.

Nodule Distribution

To model the effect of nodule distribution, three cases were considered. Figure 10 shows a typical meshing for one of the distributions considered. All distributions had a zero mean but their standard deviations (assuming normal distributions) varied. Case A had a standard deviation of 57 units, whereas B had a standard deviation of 23 units. The standard deviation of case C was zero, as all the volume fraction was concentrated in the center.

From the results shown in Table 1, it can be seen that there are only small differences in elastic modulus for the three distribution cases. Therefore, it can be concluded that distribution of the voids contributes only slightly to the modulus. It can be noted that a nodule distribution with a higher standard deviation would be preferred, as it would contribute to a small increase in the modulus.

Tertiary Effects—Surface Irregularities

Graphite nodules in real microstructures are not smooth but exhibit surface irregularities. The effect of these irregularities on the effective modulus was examined by assuming that the surface variation corresponds to sinusoidal or sawtooth waveforms. Microscopic examination of various nodules in a well-made ductile iron microstructure revealed that the irregularity varies in amplitude, up to about 10% of the nodule radius. Two wave patterns of 22 and 34 complete sinusoidal or sawtooth waveforms around the nodule were examined. Each of these waveforms was then considered to have various amplitudes. An amplitude equal to 50% of the void radius was also studied to observe the effect of graphite shapes as seen in compacted iron.

As shown in Fig. 11, the effective modulus decreased very slightly for increasing amplitude of surface irregularity. No significant difference was observed between sinusoidal and sawtooth waveforms. The wavelength of the irregularity is also seen to have little influence. For a given wave pattern, the effective modulus decreased very slightly for amplitudes up to 10% of radius. However, for an amplitude of 50% of radius, a significant decrease can be observed. Hence, surface irregularity does not appear to have a significant effect on effective moduli for smaller amplitudes but is significant at higher amplitudes.

Table 1.
Effect of Nodule Distribution on Elastic Modulus

Distribution	Standard Deviation	Predicted Modulus
A	57	0.788
B	23	0.774
C	0	0.767

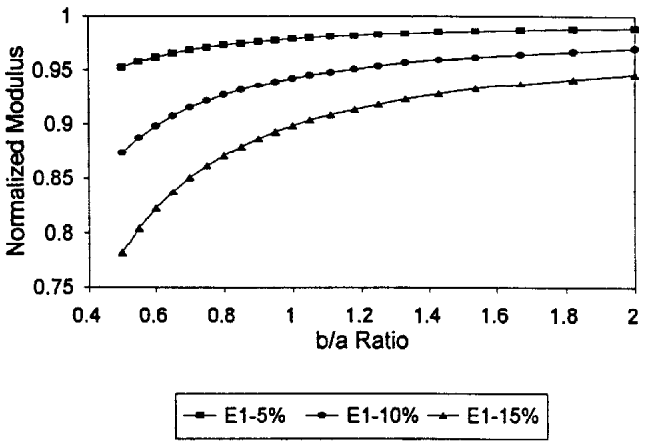

Fig. 9. Effect of ellipse axis ratio for axisymmetry.

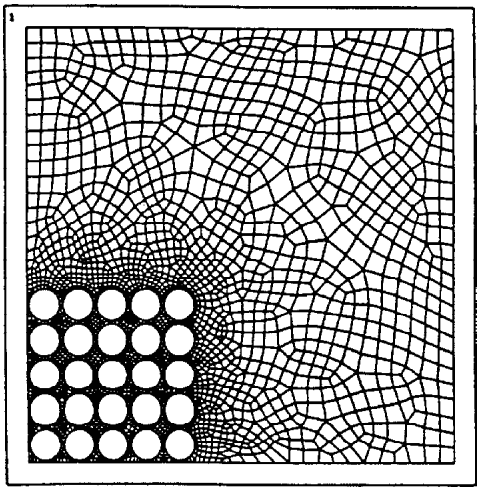

Fig. 10. Mesh used for distribution B.

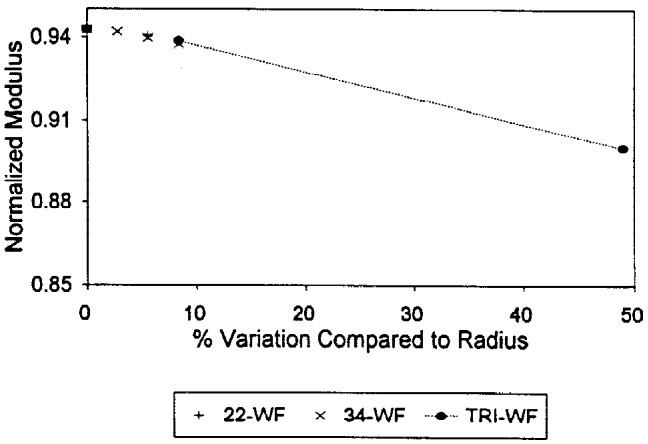

Fig. 11. Effect of surface irregularity for axisymmetry with 10% volume fraction. Waveforms (WF) are triangular or sinusoidal.

SUMMARY AND CONCLUSIONS

Finite element modeling was done to consider the effect of nodule shape, size and distribution for the same volume fraction of graphite, as this is very difficult to do either by analytical or experimental techniques. FEM was done for both plane stress and axisymmetric cases. The effective elastic modulus was calculated using the analytical method developed by Wang et al.[16] In most cases, it was assumed that graphite behaves like a void; the matrix was considered to be uniform and homogenous.

Initially, model validation was done using known literature results. The effect of volume fraction was examined, and it was seen, as expected, that the modulus decreased as the graphite volume fraction increased. Analytical modeling of the elastic modulus as a function of the volume fraction of graphite, was done considering the Rule of Mixtures, the Hashin-Shtrikman model and the Mori-Tanaka model. The Mori-Tanaka model, which was developed to predict the modulus of porous materials, gives a reasonable estimate of the observed experimental values.

The effect of nodule shape was seen for varying volume fractions as the shape changed from circular to an ellipse of increasing b/a ratio. It was seen that the modulus in the tensile Y direction increased as the orientation of the major axis of the ellipse changed from the X-axis to the Y-axis. The effect of nodule size was observed by increasing the surface area-to-volume ratio. Increases of a factor of four showed no significant variation in elastic modulus. The effect of distribution was then examined, and it was seen that nodule distribution contributes very slightly to the modulus. Surface irregularity was also modeled and was found to have no significant effect, except for very large irregularities.

INDUSTRIAL RELEVANCE

Microstructural variables, such as graphite morphology and volume fraction, are controlled in the ductile iron industry through careful control of *casting variables* such as composition, solidification and inoculation variables. The finite element study of elastic modulus in this paper is an evolutionary first step to link the critical graphite variables with casting practice using microstructure modeling.

For example, the finite element results showed clearly that graphite volume fraction and orientation have a marked effect on elastic modulus. For ductile iron foundries that have to produce castings to rigid specifications of Young's modulus, the modeling results can be used as a guide to specifying a range of carbon equivalents or nodule counts that will satisfy the customer. Another example of the industrial relevance is the implication that minor changes (up to 10% of nodule radius) in surface irregularities of graphite nodules do not greatly influence elastic modulus.

However, large irregularities, such as those caused by casting conditions that promote graphite degeneration, can significantly affect the elastic modulus. (Interestingly, increasing the surface area-to-volume ratio by increasing the nodule count (for round nodules) does not seem to affect the elastic modulus as much as changing the surface irregularities/topography.) The inference is that casting conditions that promote higher nodularity/round graphite nodules can result in increased casting stiffness, compared to imperfect or degenerate forms. Simply increasing the nodule count without sufficient spheroidization control would not be desirable. Hence, increased emphasis needs to be placed on careful selection of charge materials, and control of elements that influence the nucleation, shape and growth of the spherulites during solidification, such as Mg, Ce, Sb, As, Ti, Pb, etc.

With the great demand for higher quality castings in the ductile iron industry, these results point the way to an understanding of the role that intermediate graphite shapes (flake, quasi flake, vermicular, chunky, compacted and rosette) play in affecting elastic modulus, without conducting time-consuming expensive experimental or empirical studies. While the finite element study in this paper was limited to a study of simulated graphite variables in a homogeneous matrix, the study could be extended to include other matrix variables such as phase type and distribution, grain boundaries and segregation.

ACKNOWLEDGMENTS

The authors would like to acknowledge the support of the Natural Sciences and Engineering Research Council of Canada and the University of New Brunswick. Also to be thanked are P. Kielczynski and J. Goszczynski at the New Brunswick Research and Productivity Council.

REFERENCES

1. B. Kovacs; *Modern Casting*, pp 38-41 (Jul 1990).
2. A. Behravesh; "Mechanical and Microstructural Properties of Low Carbon Equivalent Austempered Ductile Iron," M.Sc.E. Thesis, University of New Brunswick, Fredericton, NB, Canada (1993).
3. H. Ledbetter; "Dynamic vs. Static Moduli: A Case Study," *Materials Science and Engineering*, vol A165, L9-L10 (1993).
4. A. Wolfenden, W.R. Schwanz; "An Evaluation of Three Methods to Measure the Dynamic Elastic Modulus of Steel," *Journal of Testing and Evaluation*, vol 23, No. 3, pp 176-179 (May 1995).
5. E. Plenard; "The Elastic Behavior of Cast Iron," *Recent Research on Cast Irons*, Ed. H. Merchant, pp 707-793 (1968).
6. G.R. Speich, A.J. Schwoeble, B.M. Kapadia; "Elastic Moduli of Gray and Nodular Cast Iron," *Journal of Applied Mechanics*, vol 47, pp 821-826 (1980).
7. J. Shi, S. Zou, R.W. Smith, J.J.M. Too; "Effect of Elongated Graphite on

Mechanical Properties of Hot-Rolled Ductile Iron," *Journal of Materials Engineering and Performance*, vol 3, pp 657-663 (1994).
8. B. Kovacs, G.S. Cole; "Quality Control and Assurance by Sonic Resonance in Ductile Iron Castings," *AFS Transactions*, vol 85, pp 497-501 (1977).
9. L.Y. Fang, C.R. Loper; "Development of a High Modulus Graphitic Cast Iron," *AFS Transactions*, vol 100 (1992).
10. *Ductile Iron Handbook;* American Foundrymen's Society, Des Plaines, IL (1992).
11. J.R. Dryden, A.S. Deakin, G.S. Purdy; "Elastic Analysis of Deformation near a Spherical Carbon Particle Embedded in Iron," *Acta Metallurgica*, vol 35, No. 3, pp 681-689 (1987).
12. E. Era, K. Kishitake, K. Nagai, Z. Zhang; "Elastic Modulus and Continuous Yielding Behavior of Ferritic Spheroidal Graphite Cast Iron," *Material Science and Technology*, vol 8, pp 257-261 (Mar 1992).
13. P. Dierickx, C. Verdu, A. Reynaus, R. Fougeres; "A Study of Physico-Chemical Mechanisms Responsible for Damage of Heat Treated and As-Cast Spheroidal Graphite Cast Irons," *Scripta Materialia*, vol 34, No. 2, pp 261-268 (1996).
14. Z. Hashin, S. Shtrikman; "A Variational Approach to the Theory of the Elastic Behavior of Multiphase Materials," *Journal of Mechanics and Physics of Solids*, vol 11, pp 127-140 (1963).
15. T. Mori, K. Tanaka; "Average Stress in Matrix and Average Elastic Energy of Materials with Misfitting Inclusions," *Acta Metallurgica*, vol 21, pp 571-574 (1973).
16. X.M. Wang, C.Q. Chen, Y.P. Shen; "A Method of Solution for Effective Modulus for Periodic Distributed Voids," *International Journal of Fracture*, vol 63, pp 75-80 (1993).
17. Y.L. Shen, M. Finot, A. Neddleman, S. Suresh; "Effective Elastic Response of Two-Phase Composites," *Acta Metallurgica and Materialia*, vol 42, No. 1, pp 77-97 (1994).